1



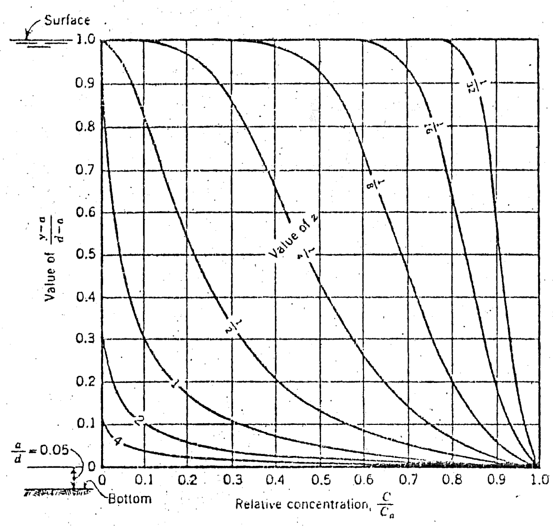


**FIG. 2.32.—Graph of Rouse Suspended Load Distribution Equation for $a/d = 0.05$ and Several Values of $z$**



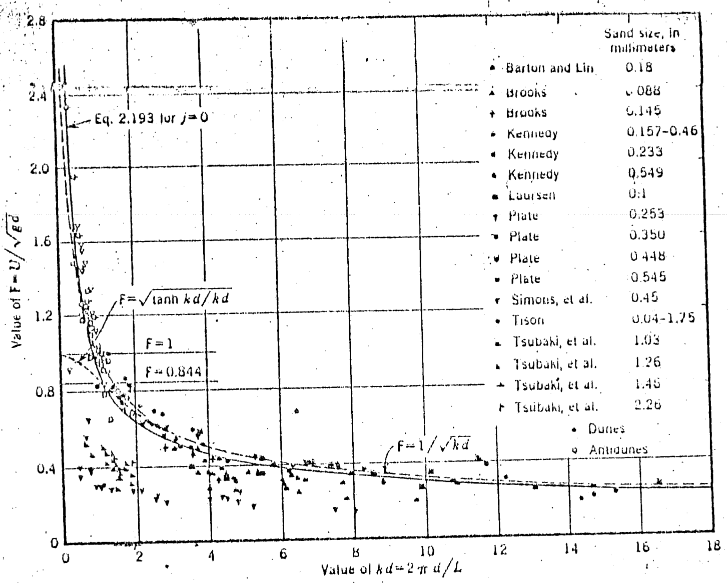


**FIG. 2.78.—Comparison of Predicted and Observed Bed Forms; Kennedy (1963)**



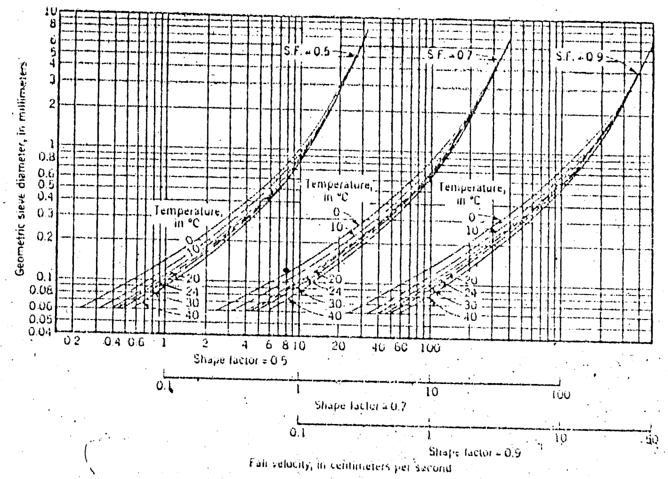


**FIG. 2.9.—Relation between Sieve Diameter, Fall Velocity, and Shape Factor for Naturally Worn Quartz Sand Particles Falling in Distilled Water (Interagency Committee, 1957)**

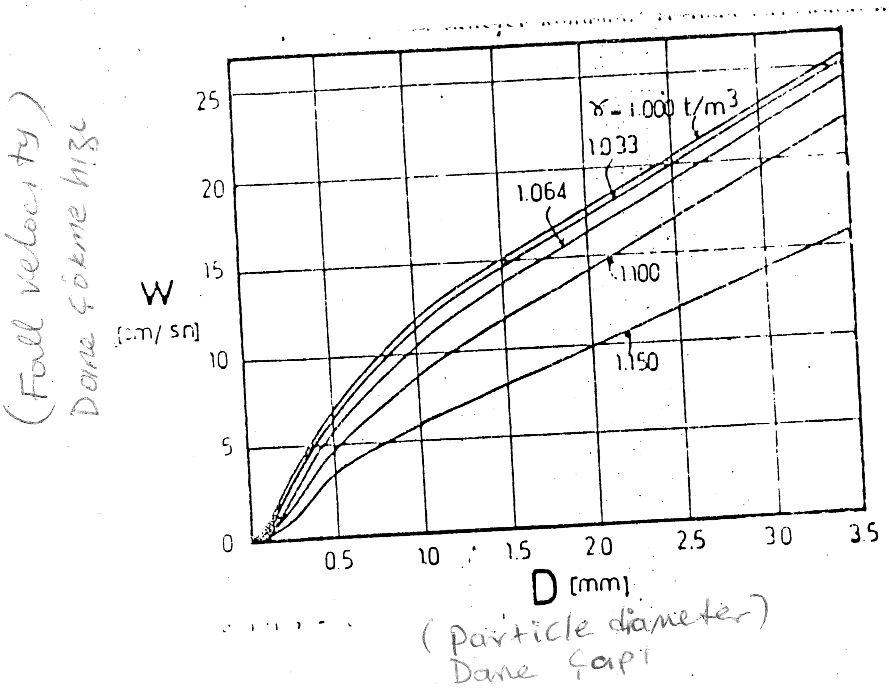

(Fall velocity)
Dane çökme hızı
W
[cm/sn]
25
20
15
10
5
0
γ = 1.000 t/m3
1.033
1.064
1.100
1.150
0.5
1.0
1.5
2.0
2.5
3.0
3.5
D [mm]
(particle diameter)
Dane çapı


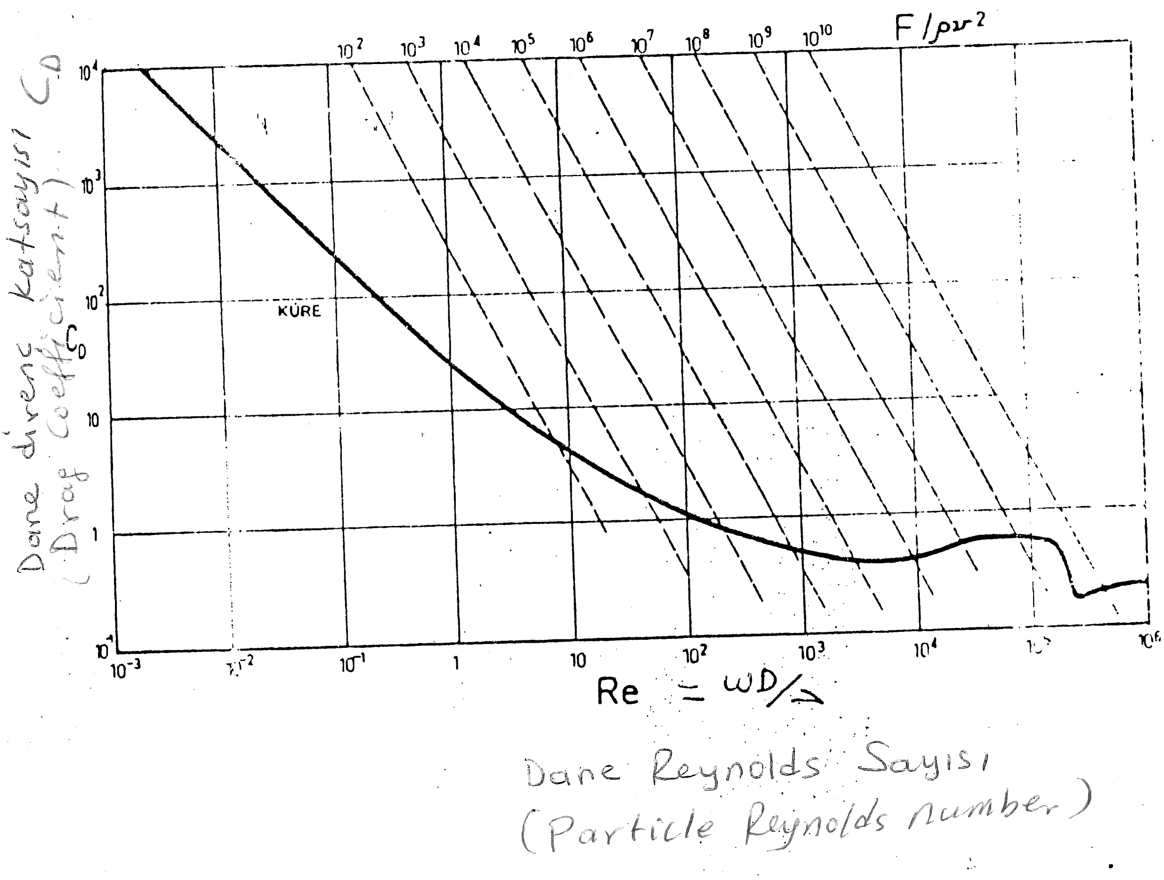

Dane direnç katsayısı $C_D$
(Drag coefficient)
$C_D$
KÜRE
$10^2$ $10^3$ $10^4$ $10^5$ $10^6$ $10^7$ $10^8$ $10^9$ $10^{10}$ $F/\rho\nu^2$
$10^4$
$10^3$
$10^2$
10
1
$10^{-1}$
$10^{-3}$ $10^{-2}$ $10^{-1}$ 1 10 $10^2$ $10^3$ $10^4$ $10^5$ $10^6$
Re $= wD/\nu$
Dane Reynolds Sayısı
(Particle Reynolds number)

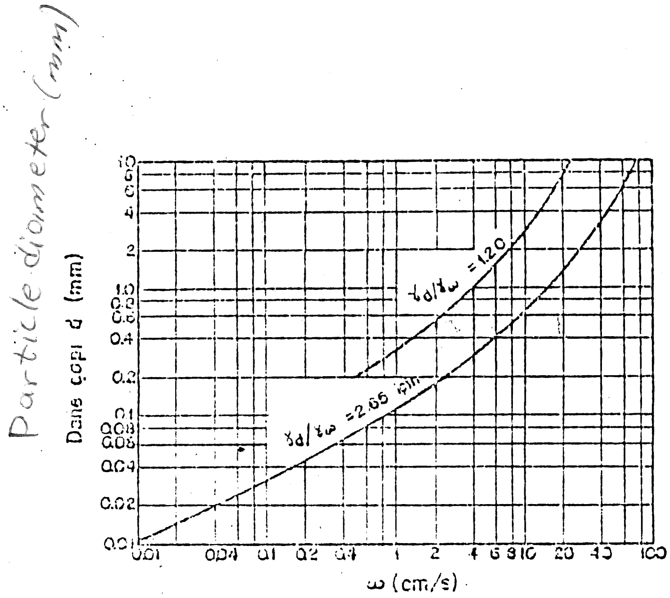


Şekil: 4.2 - küresel bir danenin çökme hızı

Fall velocity

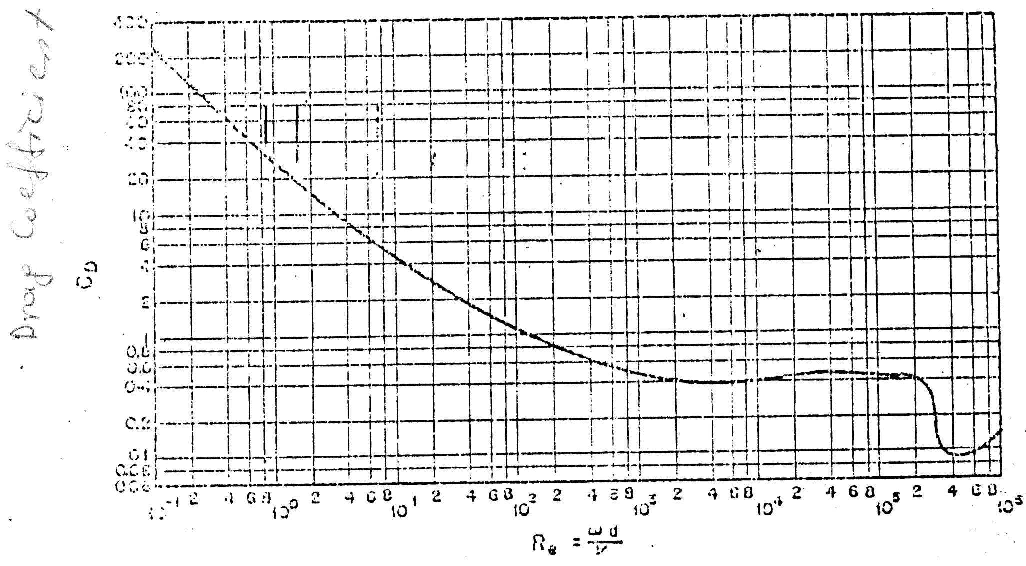


Şekil: 4.3 - Küresel bir dane için sürüklenme (direnç) katsayısının dane Reynol sayısı ile değişimi

(Particle Reynolds number)

been observed in the mean velocity of turbulent flows near the bed and ... the shear stress is approximately proportional to the local velocity squared, pulses of shear stress that have more than twice the average intensity are to be expected. White concluded that the true critical shear stress required to move a particular grain has a fixed value and that this value is given by the experiments with laminar flow. His equation for $\tau_c$ for sediment in a horizontal bed is

$$\tau_c = 0.18\,(\gamma_s - \gamma)\,d_s \tan\theta \qquad (2.107)$$

in which the constant is obtained from the experiments with laminar flow.

If it is assumed that initiation of motion is determined by $\tau_c$, $\gamma_s - \gamma$, $d_s$ and the density $\rho$ and viscosity $\mu$ ~ of the fluid, dimensional analysis immediately yields

$$\frac{\tau_c}{(\gamma_s - \gamma)d_s} = f\left(\frac{U_{*c}d_s}{\nu}\right) \qquad (2.108)$$

in which $U_{*c} = \sqrt{\tau_c/\rho}$; $\nu = \mu/\rho$; and $f$ denotes function of. This result was obtained by Shields (1936) by a much less direct method. The left-hand member of Eq. 2.108 will be called the dimensionless critical shear stress and denoted by $\tau_{*c}$ and the variable on the right is called the critical boundary Reynolds number and denoted by $R_{*c}$. When values of bed shear stress $\tau_o$, other than $\tau_c$ are used in the two quantities they are termed dimensionless shear stress and boundary Reynolds number, and are denoted by $\tau_*$ and $R_*$, respectively.

Fig. 2.43 is a graph of the data used by Shields to determine the function of Eq.

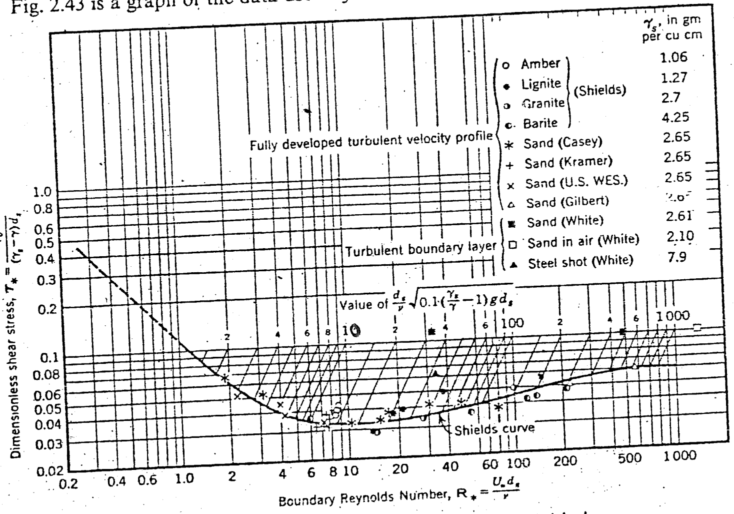


FIG. 2.43.—Shields Diagram with White Data Added

in which $\rho_s$ and $\rho$ = the densities of the sediment and fluid, ... they sought among data obtained from natural streams in California and the Missouri basin a relation between $\psi'$ and $V/U''_*$, and obtained the result

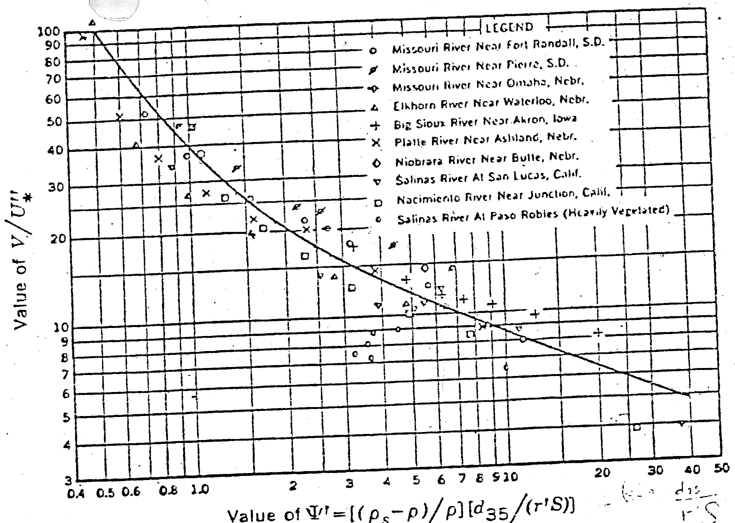


FIG. 2.56.—Einstein-Barbarossa (1952, Fig. 3) Bar Resistance Graph

1. Calculate R and $f$ from the experimental data, and compute R/$f$, which from Eq. 2.183 equals $R_w/f_w$.
2. Obtain $f_w$ from Fig. 2.68.
3. Calculate $f_b$ from Eq. 2.181.
4. Calculate $r_b = (A_b/p_b)$ from Eq. 2.177.
5. Calculate the bed shear velocity, $U_{*b} = \sqrt{g r_b S}$.
6. The bed shear stress is given by $\tau_b = \rho U_{*b}^2$.

Despite its several obvious deficiencies (division of the cross section into two noninteracting parts, determination of friction factors for section components on

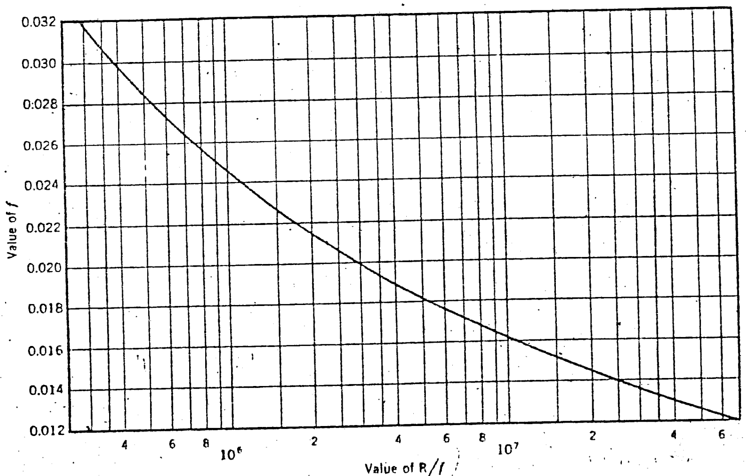


Vanoni Brooks diagram

FIG. 2.68.—Friction Factor as Function of R/$f$ for Smooth Boundary Channels and Conduits, for Use in Side-Wall Correction Calculation (Vanoni and Brooks, 1957)

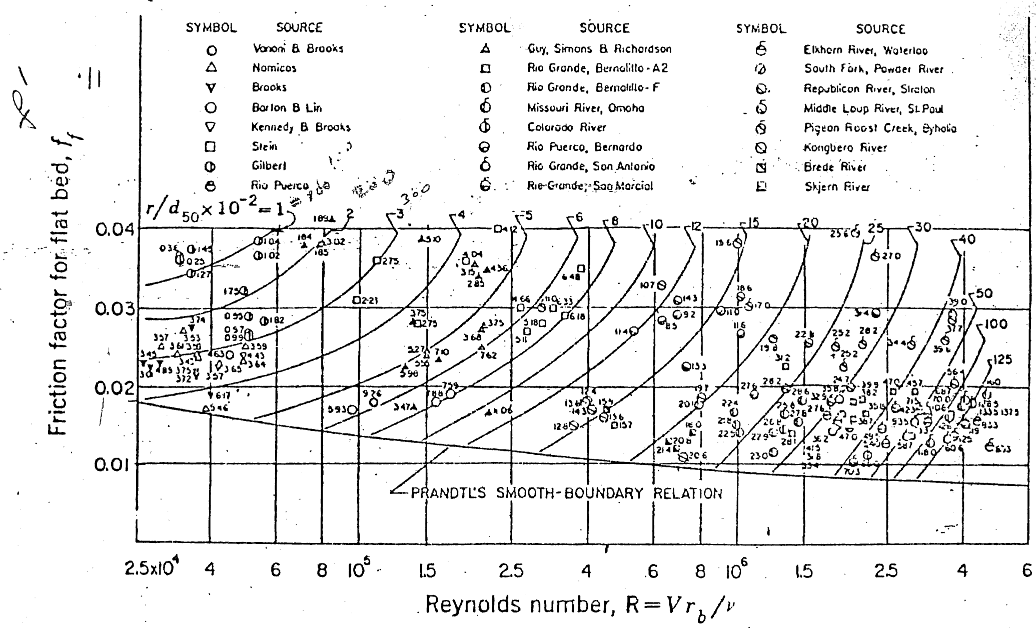


**FIG. 2.61.—Lovera and Kennedy's (1961, Fig. 1) Flat Bed Friction Factor Diagram for Alluvial Streams**

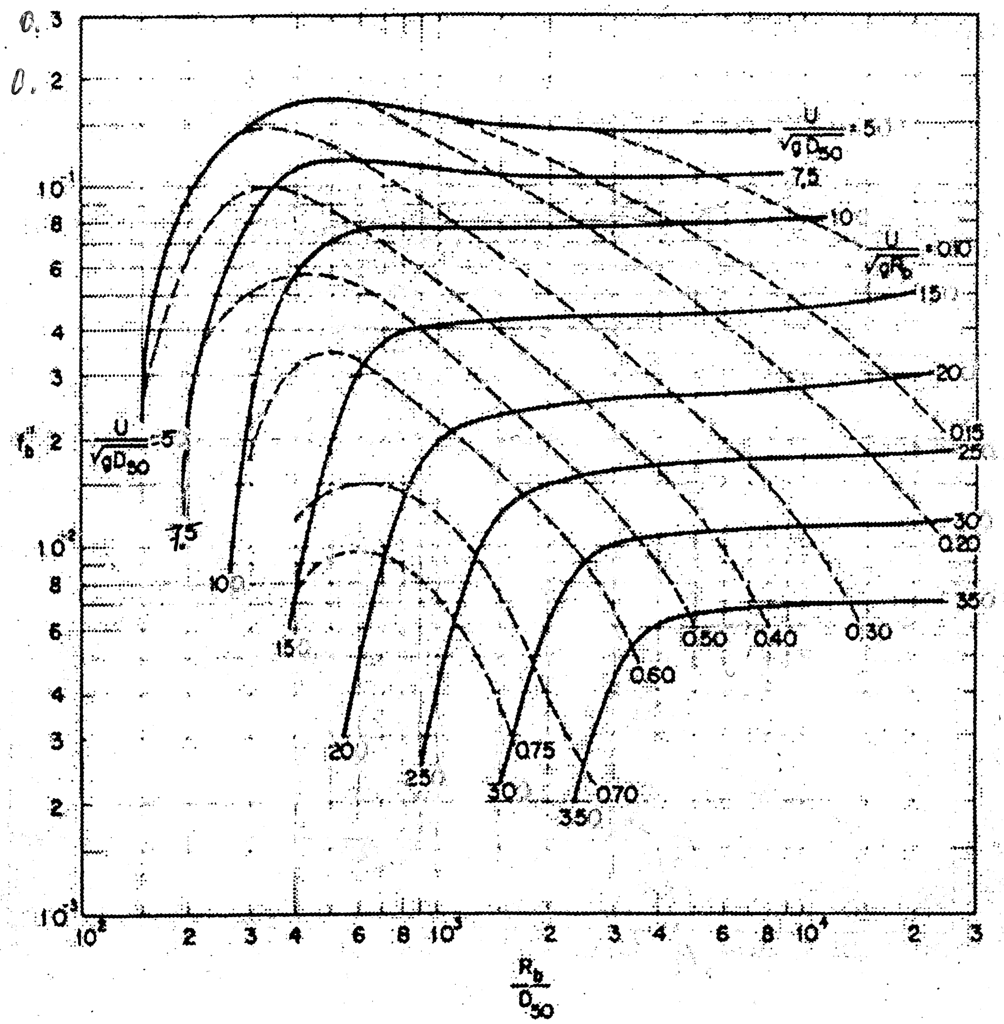


FIG. 2.62.—Alam and Kennedy's (1964, Fig. 3) Graphical Expression of $f_b''$ as Function of Froude Number and $r_b/d_{50}$

SEDIMENT TRANSPORTATION MECHANICS

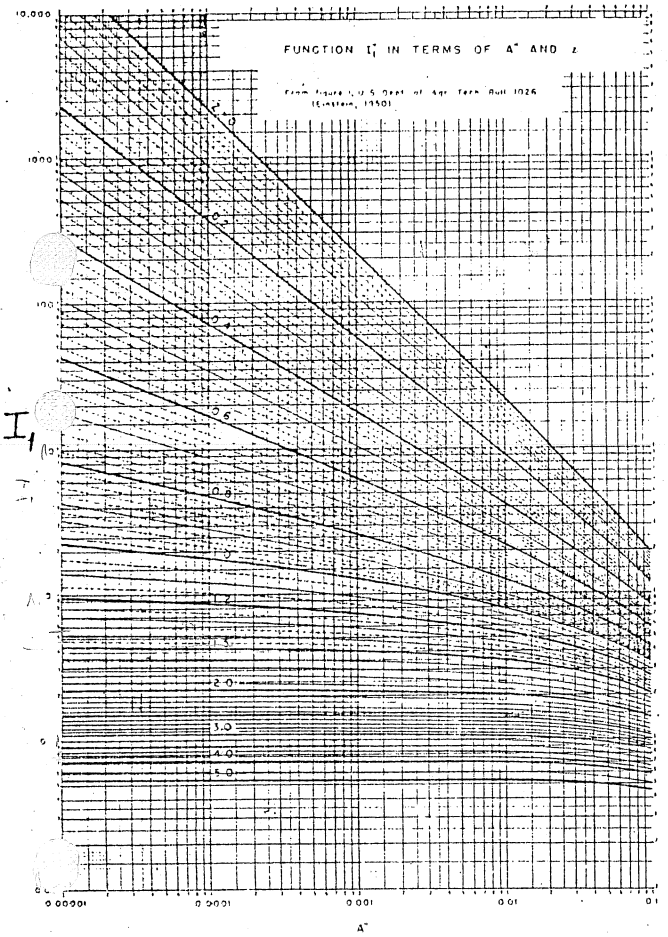


FIG. 2.98.—Integral $I_1$ in Terms of Exponent $z$ and Lower Limit $\eta_{oi}$; Einstein (1950) ($A'' \equiv 2\,d_{si}/r_b = \eta_{oi}$)

$$= \int_{d_i}^{r_b} C_i U dy \quad (2.230h)$$

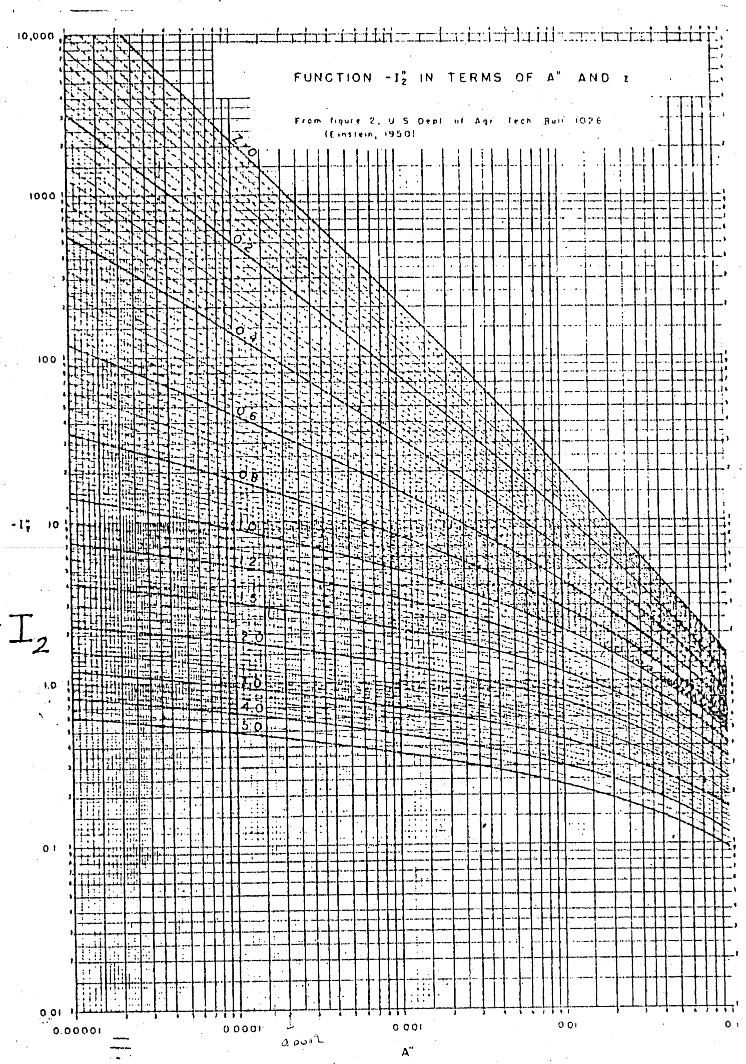


FIG. 2.99.—Integral $I_2$ in Terms of Exponent $z$ and Lower Limit $\eta_{oi}$; Einstein (1950) ($A'' \equiv 2d_{si}/r_b = \eta_{oi}$)

SEDIMENT TRANSPORTATION MECHANICS

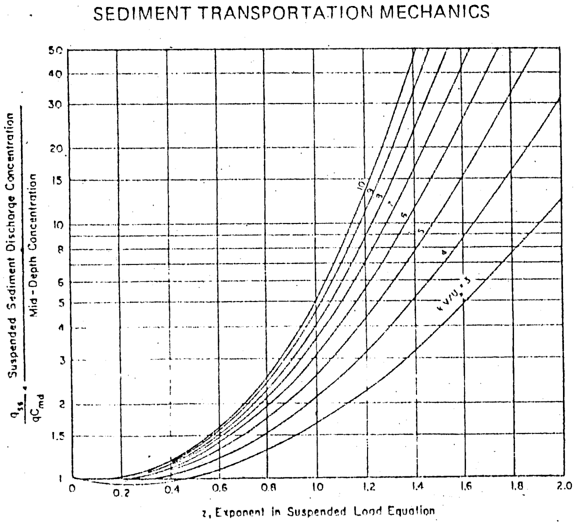


. 2.84.—Chart for Determining Suspended-Sediment Discharge, $g_{ss}$, from Known ues of $kV/u_*$, Exponent $z$, and Mid-Depth Concentration $C_{md}$; Brooks (1965)

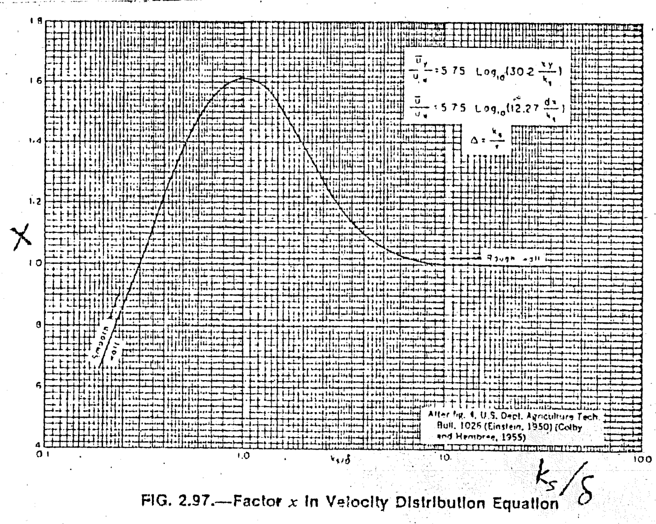


FIG. 2.97.—Factor $x$ in Velocity Distribution Equation

6

Einstein
Bed load
Suspended load



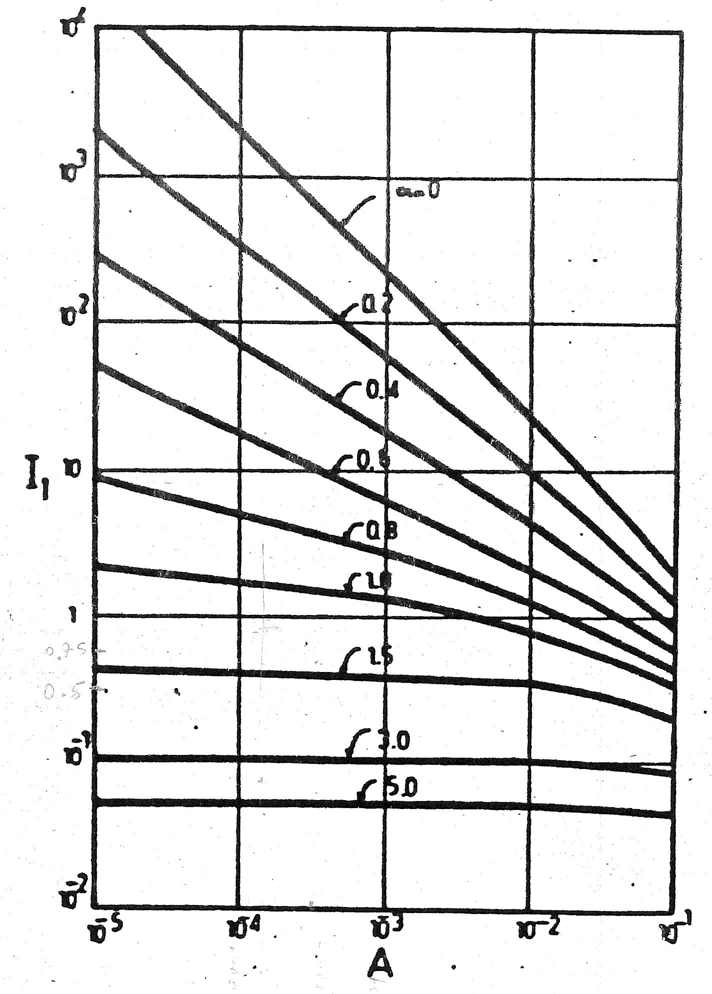


Şekil 6.7.a . (6.21) denklemindeki $I_1$ büyüklüğünün $A$ ve α ya bağlı olarak değişimi [ 6.2 ] .

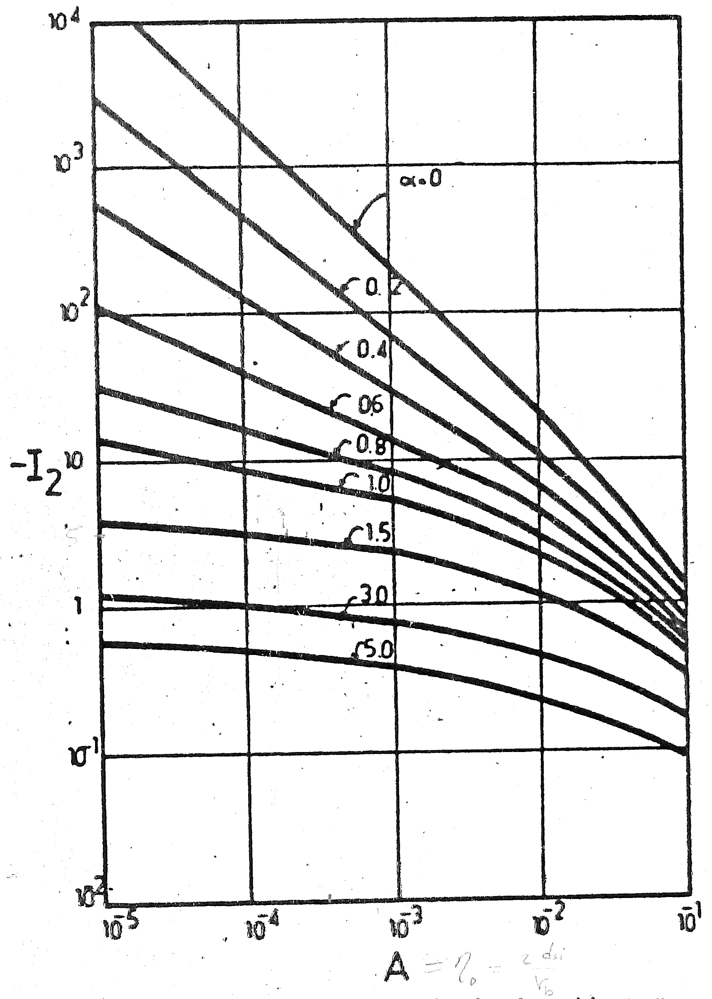


Şekil 6.7.b. (6.21) denklemindeki $I_2$ büyüklüğünün $A$ ve α ya bağlı olarak değişimi [ 6.2 ] .

Prot. (K-49-2?)

# VANONİ - BROOKS DİYAGRAMI

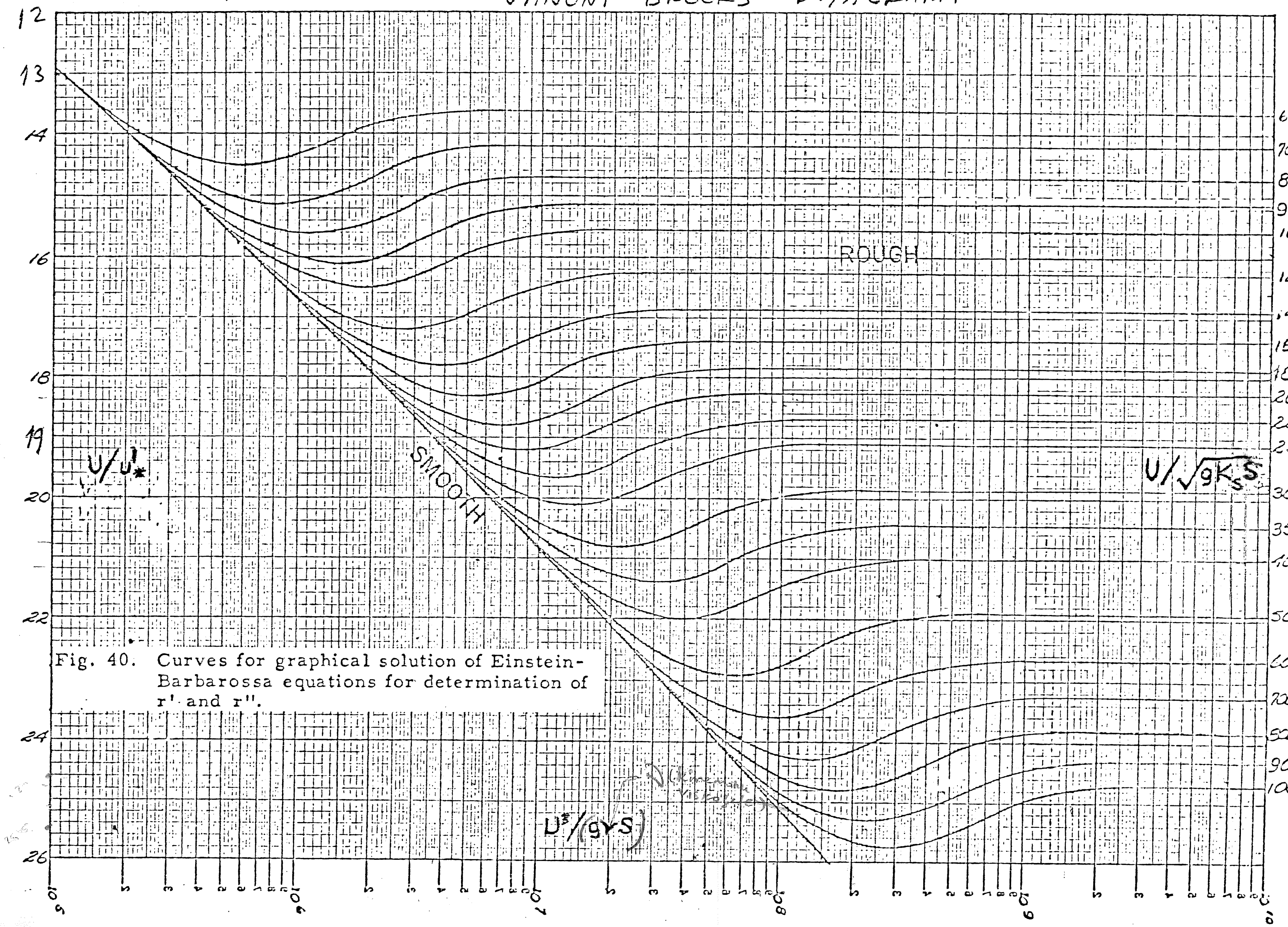


Fig. 40. Curves for graphical solution of Einstein-Barbarossa equations for determination of r' and r''.

Nevzat Yıldırım

7

The relation for $g_{sbi}$ remaining to complete the Einstein theory is the actual Einstein Bed Load Function

$$1 - \frac{1}{\sqrt{\pi}} \int_{-(1/7)\Psi_{*i}-2}^{(1/7)\Psi_{*i}-2} e^{-t^2}\,dt = \frac{43.5\Phi_{*i}}{1 + 43.5\Phi_{*i}} \qquad \text{(2.230j)}$$

in which $$\Psi_{*i} = \xi_i Y \left( \frac{\log 10.6}{\log \dfrac{10.6x\,X}{d_{65}}} \right)^2 \frac{(\gamma_s - \gamma) d_{si}}{\gamma r_b' S} \qquad \text{(2.230k)}$$

$$\Phi_{*i} = \frac{1}{p_i} \frac{g_{sbi}}{\gamma_s} \sqrt{\left( \frac{\gamma}{\gamma_s - \gamma} \right) \frac{1}{g d_{si}^3}} \qquad \text{(2.230l)}$$

In these equations $\xi_i$ = a function of $d_{si}/X$ given in Fig. 2.100; $Y$ = a function of $d_{65}/\delta$ given in Fig. 2.101

$$\left. \begin{aligned} X &= 0.77 \frac{d_{65}}{x} \text{ when } \frac{d_{65}}{x\delta} > 1.80 \\ X &= 1.398\,\delta \text{ when } \frac{d_{65}}{x\delta} < 1.80 \end{aligned} \right\} \qquad \text{(2.230m)}$$

$$\delta = 11.6 \frac{\nu}{U'_*} \qquad \text{(2.230n)}$$

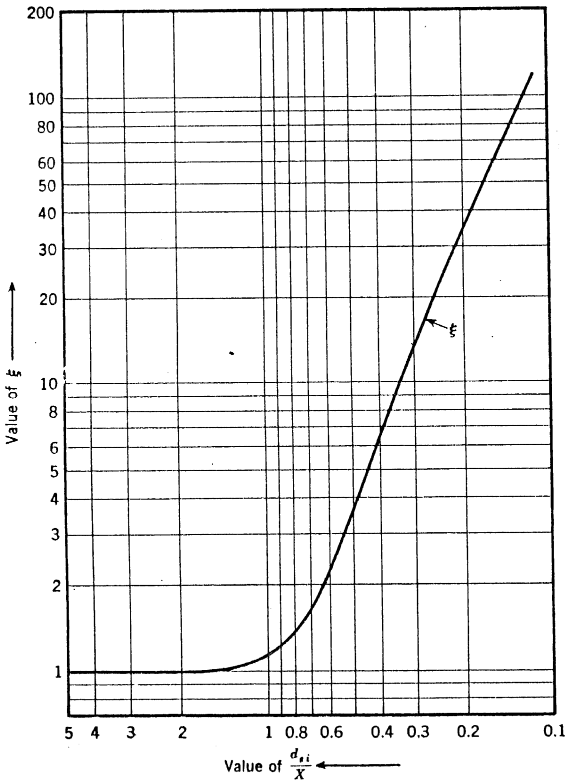


**FIG. 2.100.—Factor $\xi$ in Einstein's Bed Load Function (Einstein, 1950) in Terms of $d_{si}/X$**

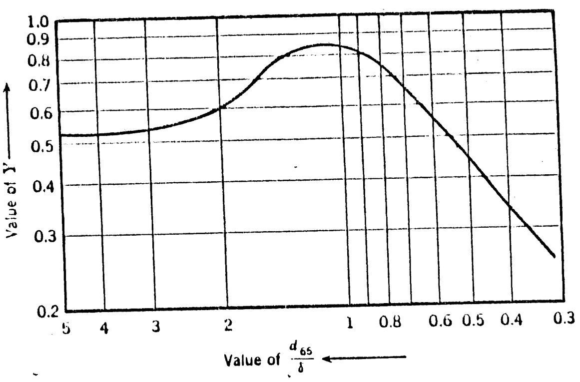


**FIG. 2.101.—Factor $Y$ in Einstein's Bed Load Function (Einstein, 1950) in Terms of $d_{65}/\delta$**

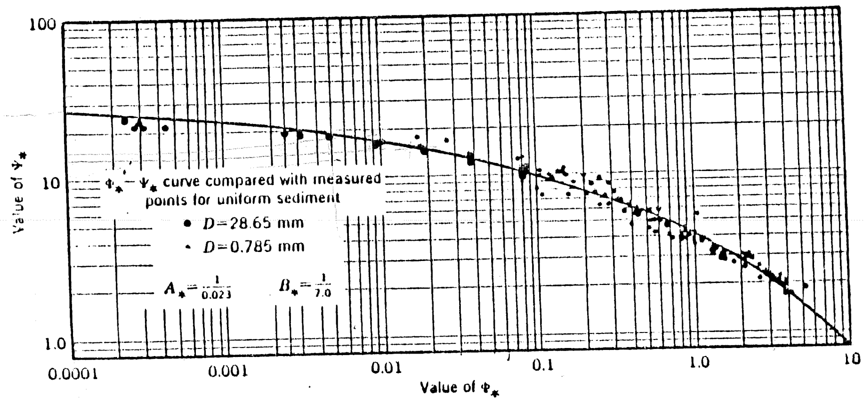


**FIG. 2.102.—Einstein's $\Phi_* - \Psi_*$ Bed Load Function (Einstein, 1950)**

Term $r_b'$ is the Einstein-Barbarossa bed hydraulic radius corresponding to the sand grain resistance of the bed and is determined as described in Chapter II, Section F. For bed sediment of uniform size, $X = 1.39\delta$ and $Y = 1.0$.

As already stated Eq. 2.230j is the Einstein bed load function that gives the bed load discharge, $g_{sbi}$. Fig. 2.102 gives the bed load function, i.e., $\Phi_*$ as a function of $\Psi_*$. This result then enables one to calculate the suspended-sediment concentration, $C_{ai}$, at a distance, $2\,d_{si}$, above the bed by means of Eq. 2.230i.

Calculation of the sediment discharge of a stream by the Einstein bed load function can be carried out in three parts. The first part involves collecting field data that include measurements of: (1) Slope; (2) data on cross section from which one can determine the bed width and the cross-sectional area and wetted perimeter of the banks as functions of depth; (3) a representative sample of the bed sediment; (4) a mechanical analysis of the bed sample from which the weight fraction, $p_i$, can be determined for each size, $d_{si}$, and values of $d_{35}$ and $d_{65}$ can be read; and (5) an estimate of the friction factor of the channel banks.

In the second part, calculations are made to determine values of the bed hydraulic radius, $r_b'$, due to sand grain roughness for a range of values of water discharge $Q$. Such calculations are described in Chapter II, Section F.

SLURRY FLOW



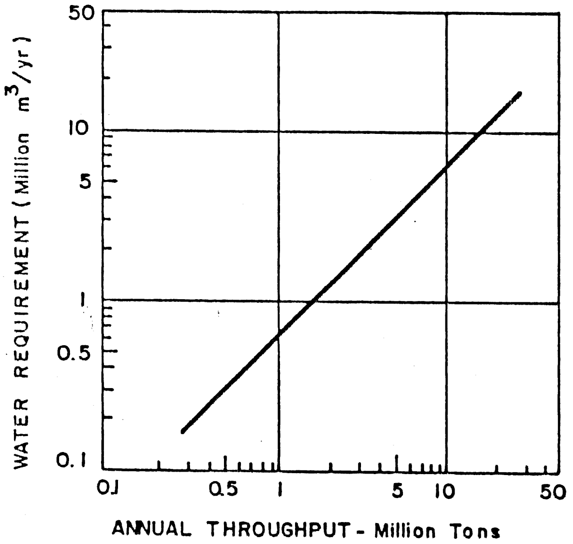


FIG 1- WATER REQUIREMENTS FOR SLURRY PIPELINES

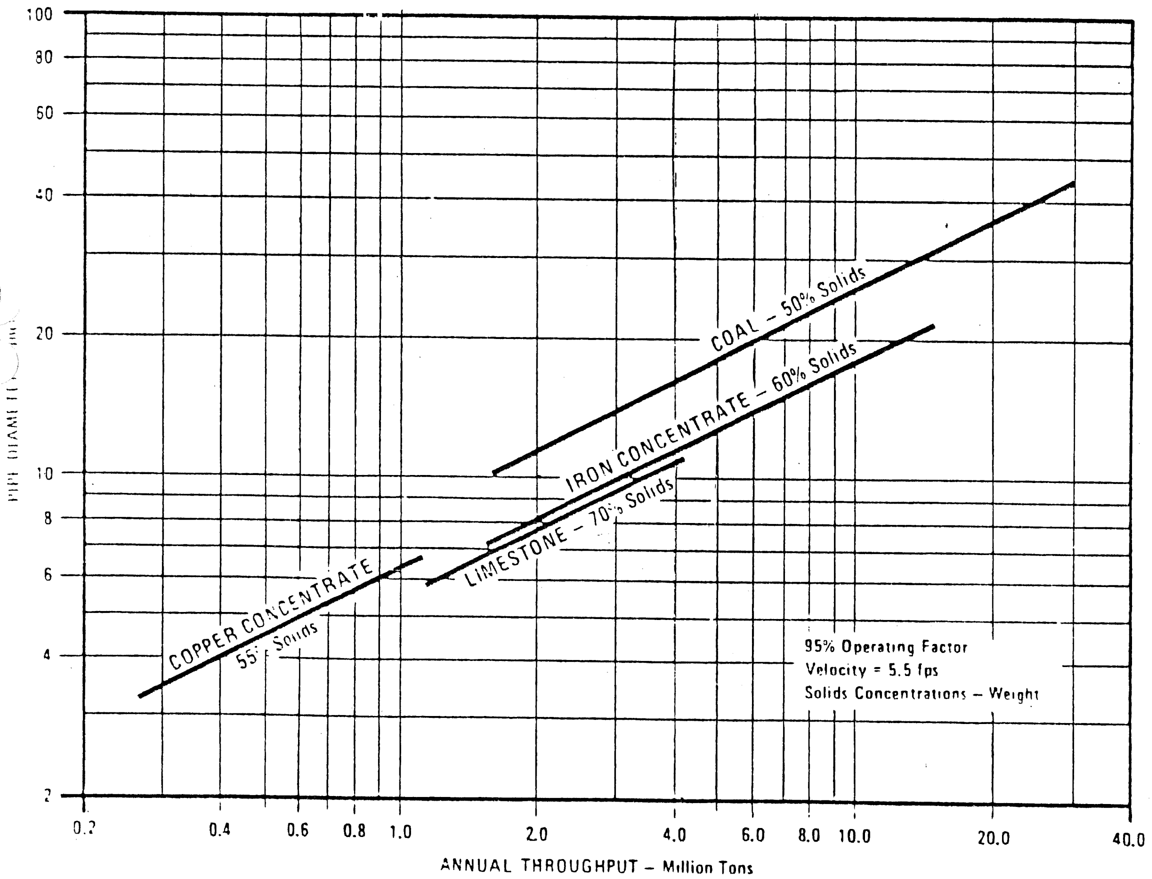


FIG 2- PIPE DIAMETER FOR SLURRY PIPELINES

SLURRY FLOW

(A)

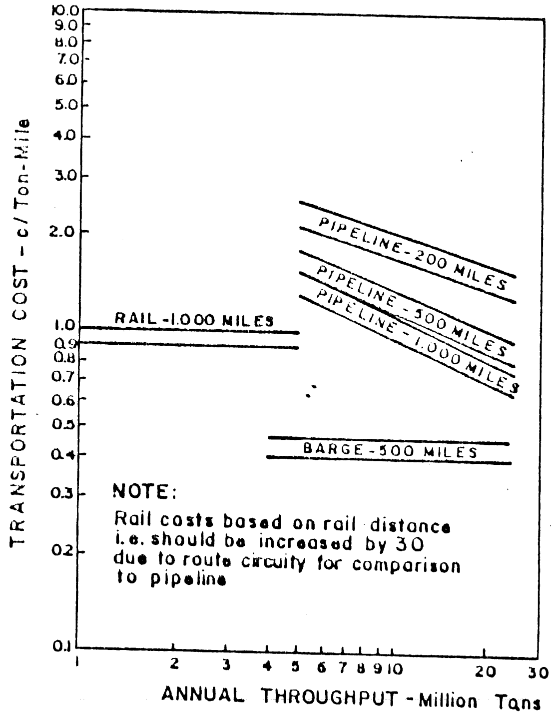


(B)

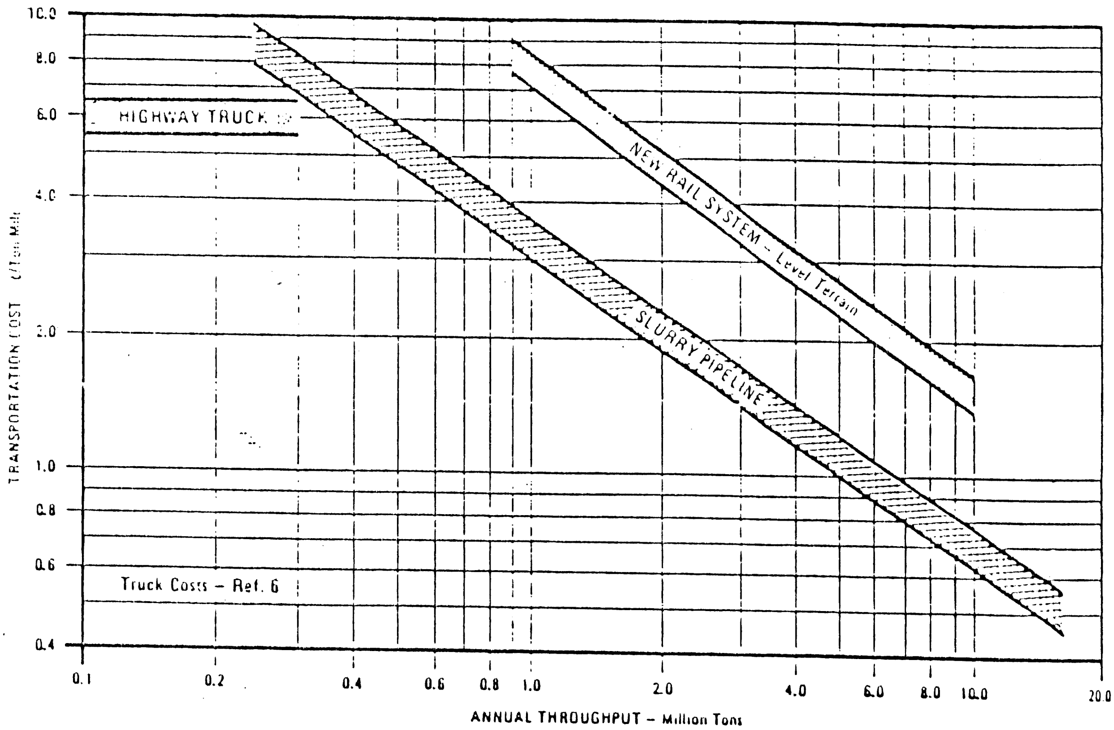


FIG 3- TRANSPORTATION COSTS (A) COAL (B) IRON,COPPER,LIMESTONE

SLURRY FLOW

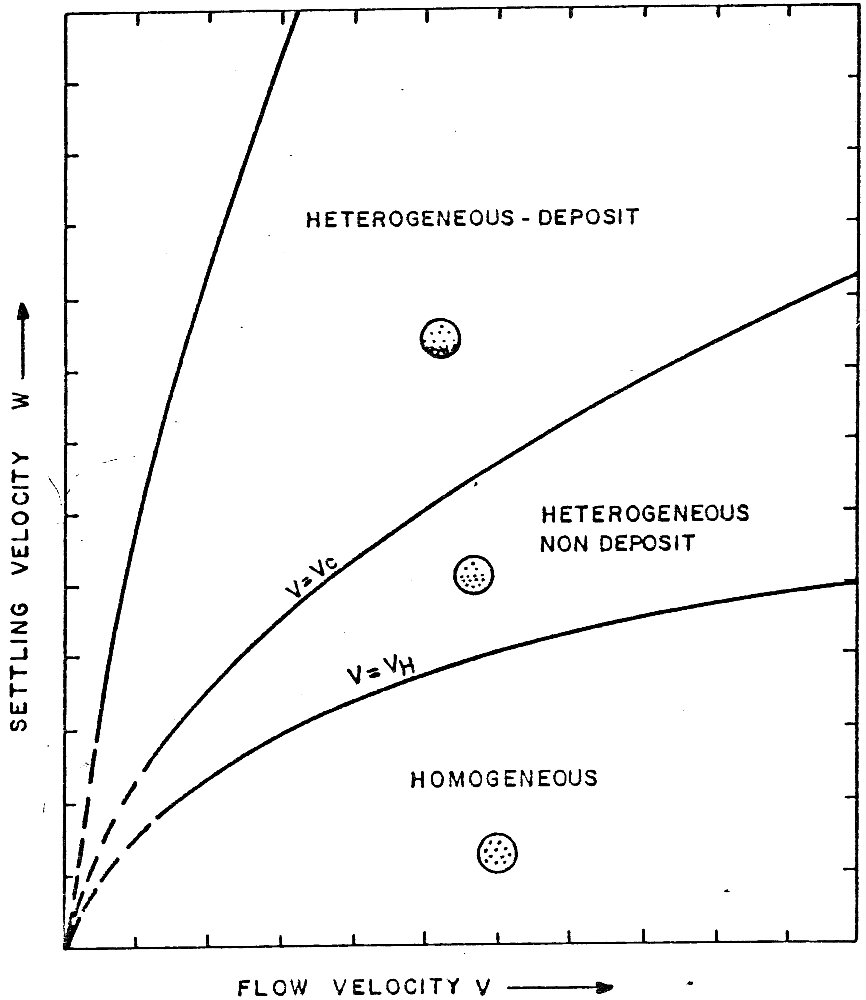


FIG 4- CLASSIFICATION OF SOLID-LIQUID FLOWS

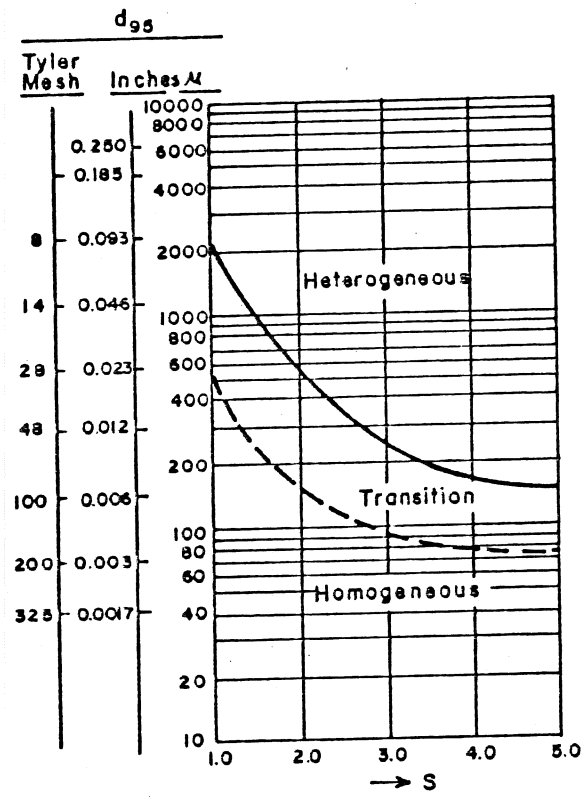


FIG 5- HOMOGENEOUS-HETEROGENEOUS FLOW REGIMES

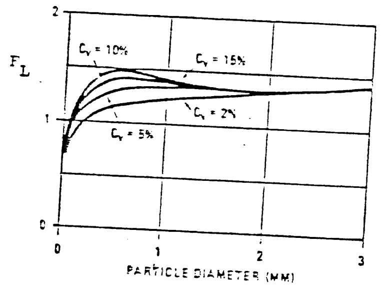


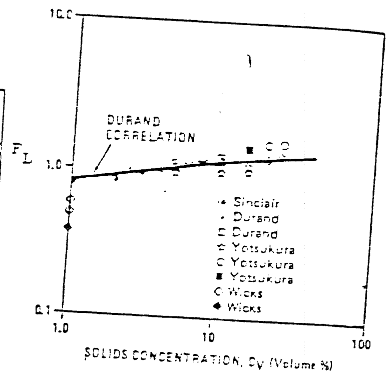


FIG -6 VARIATION OF DURAND COEFFICIENT $F_L$

For particle sizes up to 1 mm, both concentration and particle diameter have an effect on the value of $F_L$. For particles greater than 1 mm, the dependence becomes weaker, until, for large particles the value of $F_L$ is constant regardless of system properties. Thus for a given system of particles larger than say 2 mm, the critical velocity as given by Eq.4, is a function of pipe diameter alone, varying as the square root of D.

WASP et al (1970) have presented a review of the published data for critical velocities. Fig.6.b. shows a plot of $F_L$ versus solids concentration for sand-water slurries and includes data from DURAND (1952), SINCLAIR (1962), YOTSUKURA (1961) and WICKS (1968), together with the correlation line given by Eq.4 and Fig.6.a. The DURAND correlation gives excellent prediction of the data with the exception of those of WICKS, which were for low solids concentrations (one percent by volume) and a varying fluid density and viscosity.

Although the DURAND expression shows excellent agreement for sand-water slurries, it is inadequate for suspensions of coal and iron particles as reported by SINCLAIR (1962). It must be concluded, therefore, that Eq.4. does not fully describe the function of relative density as it affects critical velocity.

SLURRY FLOW



Several other experimental-empirical relations for critical velocity have been proposed, some of which are:

SPELLS (1955):

$$V_c^{1.225} = 0.025\ gd\ \left(\frac{D\ c\ m}{\mu\ m}\right)^{0.775} (s-1) \qquad (5)$$

ZANDI and GOVATOS (1967) :

$$V_c^2 = 40\ C_v\ \frac{Dg\ (s-1)}{\sqrt{C_D}} \qquad (6)$$

where $C_D$ is the drag coefficient of the particle settling in clear water.

HUGHMARK (1961) :

$$\frac{V_c}{\sqrt{gD}} = f\ (C_v\ (s-1)\ F_D\ ) \qquad (7)$$

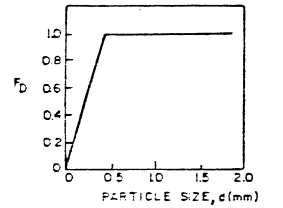


where, the function $f$ is plotted in Fig.7 and the coefficient $F_D$ which is dependent on particle size, is shown above.

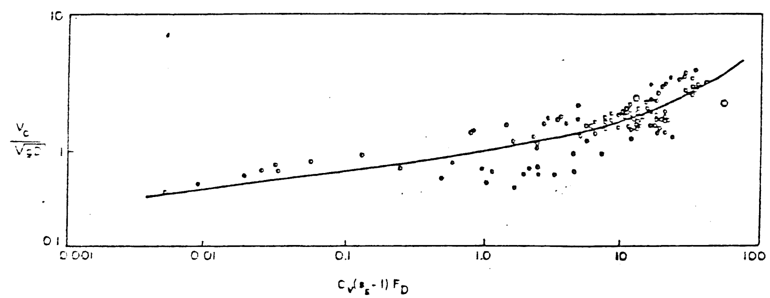


FIG 7- HUGHMARK'S FUNCTION f.

13

Slurry flow

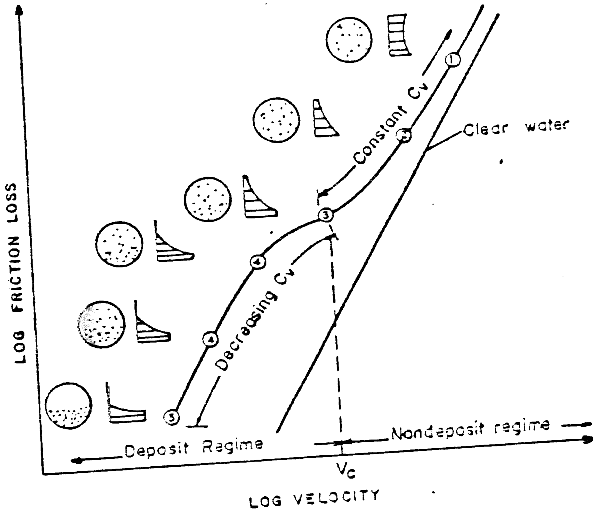


1 HOMOGENEOUS FLOW
2 HETEROGENEOUS NONDEPOSIT REGIME
3 START OF DEPOSITION
4 HETEROGENEOUS DEPOSIT REGIME
5 FIXED DEPOSIT

FIG 8- FRICTION LOSSES IN SOLID-LIQUID FLOWS

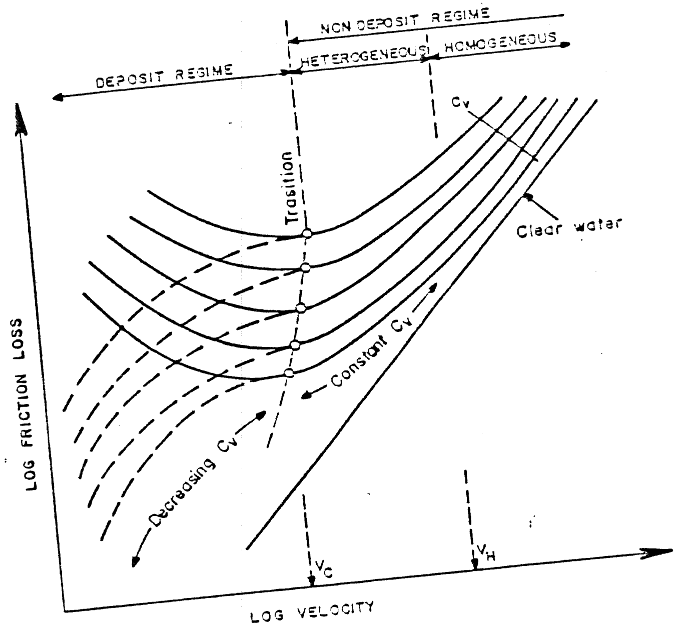


FIG 9- FRICTION LOSS WITH CONSTANT CONCENTRATION

Table 2.1 in which the maximum size in each fraction is twice the minimum size. The mean size, $d_{si}$, of each fraction is taken as the geometric mean of the maximum and minimum sizes in the fraction. The sediment discharge is taken as the sum of that for each of the fractions. The assumption is made, as by Einstein (1950), that the discharge of material in a size fraction of the bed sediment is proportional to the weight fraction, $p_i$, of the fraction.

For purposes of calculation, the depth, $r$, of the hypothetical stream is divided into the four zones shown in Fig. 2.108. These are: (1) The bed zone of relative thickness $y/r = 2\,d_{si}/r$; (2) the lower zone extending from $y/r = 2\,d_{si}/r$ to $y/r = 1/11.24$; (3) the middle zone extending from $y/r = 1/11.24$ to $y/r = 1/2.5$; and (4) the upper zone extending from $y/r = 1/2.5$ to the surface. The velocity profile is represented by the power relation

$$U = (1 + n_v)\,V\left(\frac{y}{r}\right)^{n_v} \qquad (2.236a)$$

in which $U$ = the flow velocity at the distance $y$ above the bed; $V$ = the mean velocity, in feet per second of the real stream; and the exponent, $n_v$, is given by the empirical relation

$$n_v = 0.1198 + 0.00048T \qquad (2.236e)$$

in which $T$ = the water temperature, in degrees Fahrenheit. The concentration distribution of each size fraction is given by a power relation for each of the three upper zones, i.e., by Eqs. 2.236b–d as shown in Fig. 2.108. The equations closely approximate the theoretical distribution of concentration given by Eq. 2.77. The exponent, $z_i$, in Eqs. 2.236b–d is given by

$$z_i = \frac{w_i V}{c_z r S} \qquad (2.236f)$$

in which $w_i$ = the fall velocity, in feet per second, of the sediment of size, $d_{si}$, in water at temperature $T$; $S$ = the slope of the real stream; and $c_z$ is given by the empirical equation

TOFELLETI YÖNTEMİ

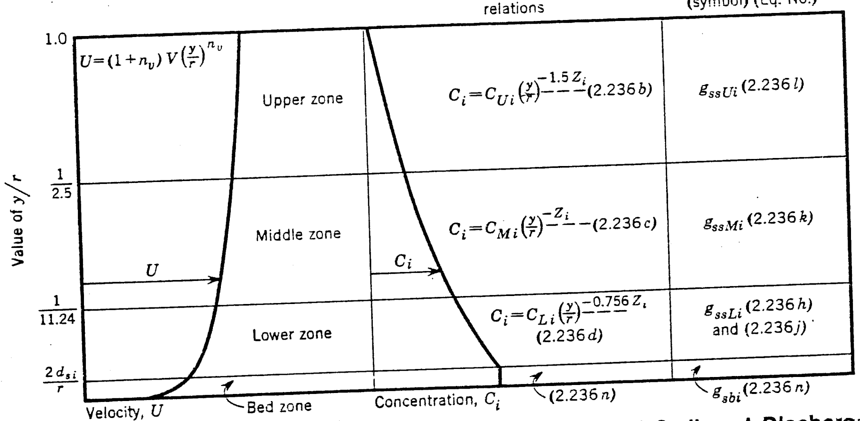


FIG. 2.108.—Toffaletti's (1969) Velocity, Concentration, and Sediment Discharge Relations



$$c_z = 260.67 - 0.667T \qquad (2.236g)$$

in which $T$ = water temperature, in degrees Fahrenheit. When the value of $z_i$ is less than $n_v$, $z_i$ shall be arbitrarily taken equal to 1.5 $n_v$. The quantities $n_v - 1.5\,z_i$ and $n_v - z_i$ appear as the exponent of $y/r$ in the product, CU, for the upper and middle zones, respectively. This arbitrary procedure assures that this exponent is never positive and that the product, CU, decreases as $y/r$ increases as it does in streams.

Expressions for the suspended load discharges, $g_{ssLi}$, $g_{ssMi}$, and $g_{gssUi}$ in the lower, middle, and upper zones, respectively, are obtained by substituting $U$ from Eq. 2.236a and the appropriate relations for $C_i$ into Eq. 2.230h and integrating between the appropriate limits. Since $C_{Ui}$ and $C_{Mi}$ in Eqs. 2.236b and 2.236c can be expressed in terms of $C_{Li}$, the sediment discharges in the three zones will all be expressed in terms of $C_{Li}$, which is still unknown. This is determined from Eq. 2.236h, an empirical equation for $g_{ssLi}$:

$$g_{ssLi} = \frac{0.600\,p_i}{\left(\frac{T_T A\,k_4}{V^2}\right)^{5/3}\left(\frac{d_{si}}{0.00058}\right)^{5/3}}\ \text{(tons/day/ft)} \qquad (2.236h)$$

in which $A$ = a function of $(10^5\nu)^{1/3}/10U'_*$ given in Fig. 2.109(a); $\nu$ = the kinematic viscosity of the water, in square feet per second; $U'_*$ = shear velocity, in feet per second based on the bed shear stress due to sand grain roughness, defined previously; and $T_T$ is given by

$$T_T = 1.10\,(0.051 + 0.00009T) \qquad (2.236i)$$

in which $T$ = water temperature, in degrees Fahrenheit. The number 0.00058 in Eq. 2.236h is the geometric mean size of fine sand expressed in feet. Therefore the sand size, $d_{si}$, in Eq. 2.236h must also be expressed in feet. The dimensions of $A$ are such that $g_{ssLi}$ in Eq. 2.236h is given in tons per day per foot of width. The factor,

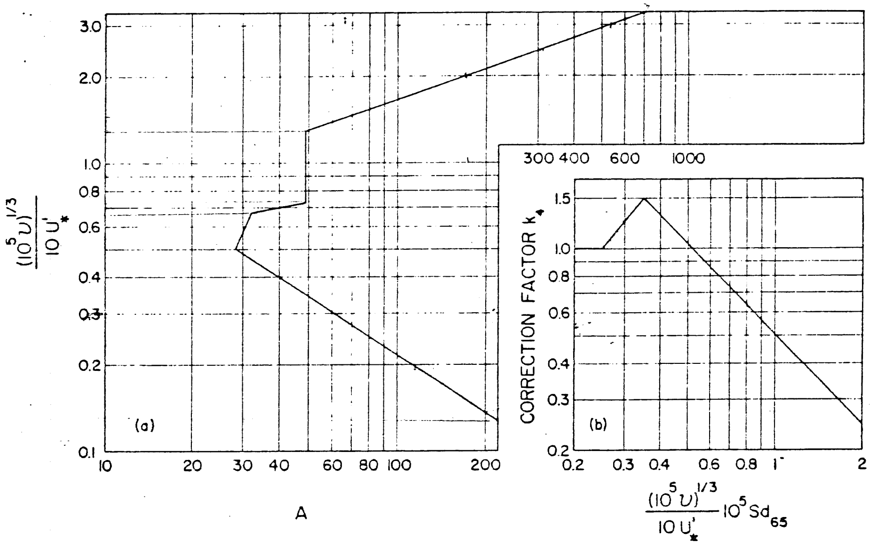


FIG. 2.109.—Factors in Toffaletti Relations: (a) Factor $A$ in Eq. 2.236h; (b) Correction Factor $k_4$ in Eq. 2.236h

15

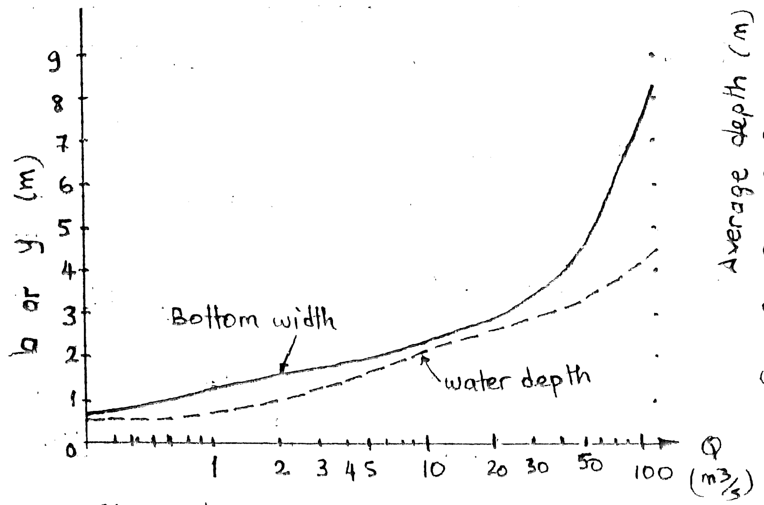


Channel dimensions for lined canals

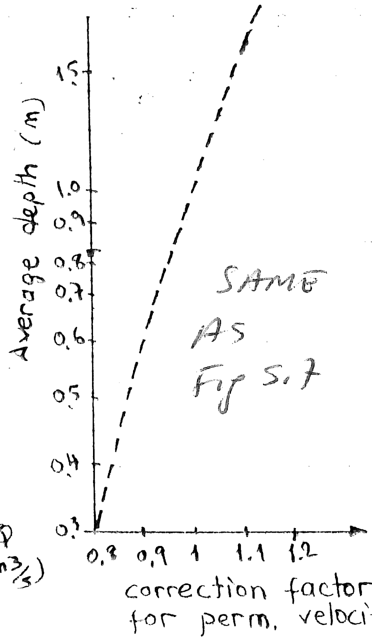


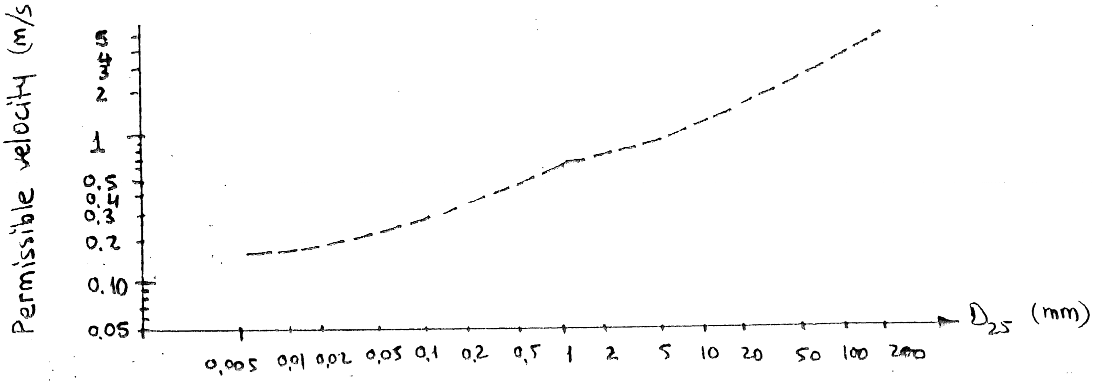


Fig. 5.5- Permissible velocity for noncohesive soils

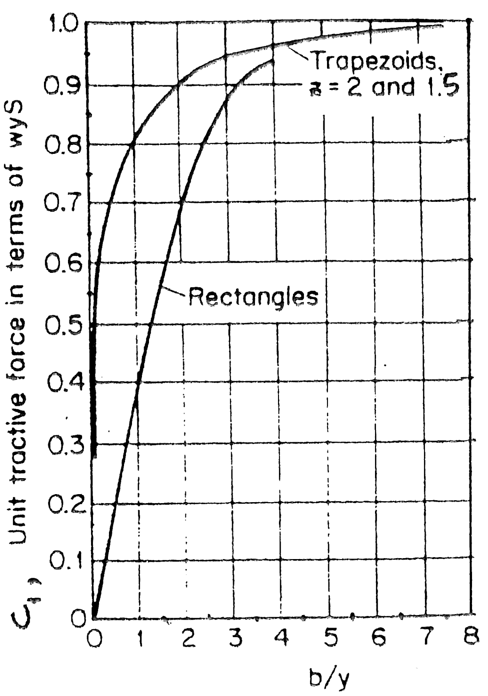


On bottom of channels

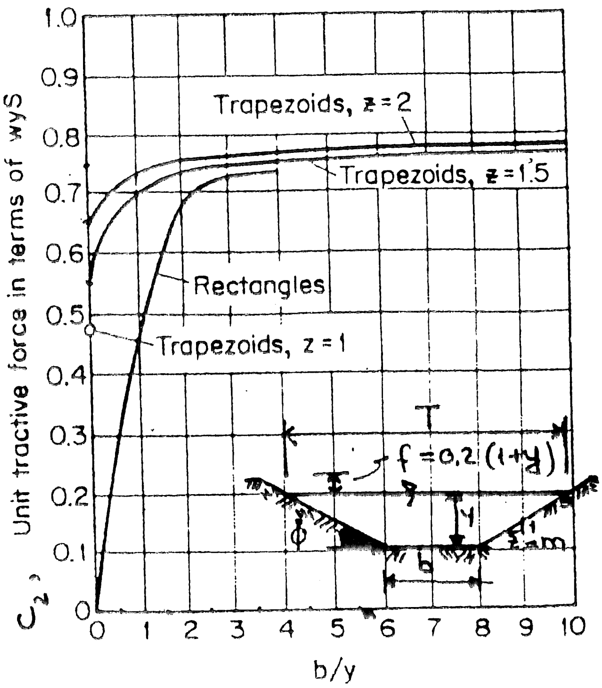


On sides of channels

Fig. 5.10

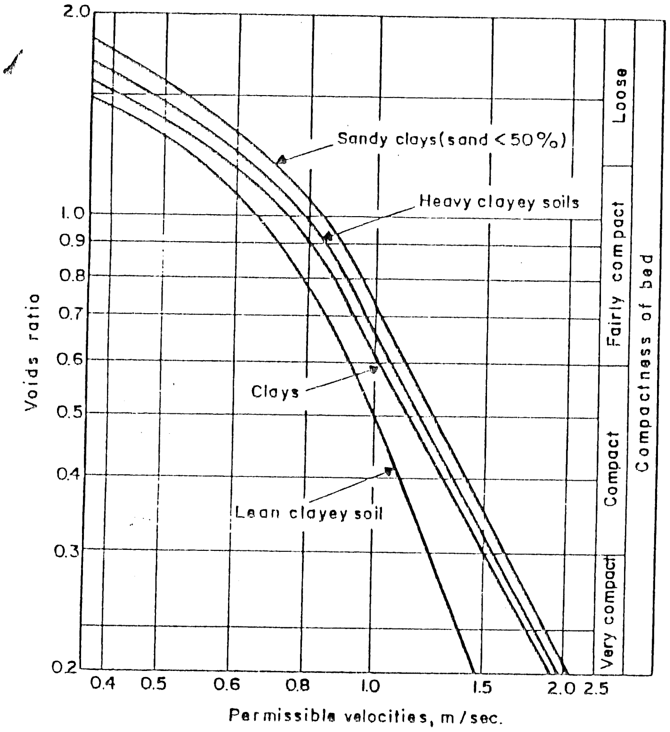


Figure 5.6. Permissible velocities for cohesive soils

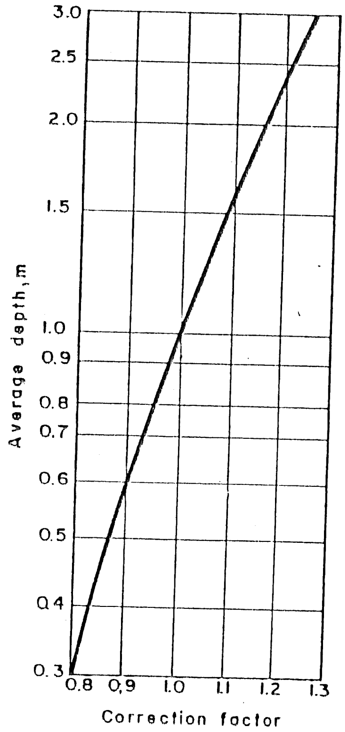


Figure 5.7. Correction factor